

## Positron annihilation in thermally quenched potassium chloride\*

S. Dannefaer, G. W. Dean, and B. G. Hogg

*Department of Physics, University of Winnipeg, Winnipeg, Canada*

(Received 16 September 1975)

Positron annihilation lifetime and Doppler-broadened spectra have been obtained for thermally quenched KCl. It is found that internal consistency between the results of the two techniques is achieved when lifetime spectra are decomposed into four components. Using a simple statistical model for the annihilation of positrons it is deduced that the formation energy of Schottky defects is  $2.1 \pm 0.2$  eV and further, that positrons trapped at vacancies have a lifetime of about 0.34 nsec. The two longest-lived components with lifetimes  $0.77 \pm 0.05$  and  $4.4 \pm 0.02$  nsec are shown to arise from annihilation of positronium. The positronium yield increases from about 16% at  $T < 150^\circ\text{K}$  to about 25% at  $T > 250^\circ\text{K}$ , the temperature region investigated being  $90\text{--}296^\circ\text{K}$ . From Doppler-broadened spectra it is deduced that positronium is confined within a space of diameter  $2 \text{ \AA}$ .

### I. INTRODUCTION

There have been many studies of the annihilation of positrons in alkali halides but still, the interpretation of the data poses several difficulties. A source of these difficulties is found in the large scatter of the lifetime results from different laboratories.<sup>1-5</sup> Furthermore, the number of decay modes present is uncertain since in some cases spectra have been analyzed successfully with a two-exponential (in the following referred to as component) fit while in others three-component fits were used. For the most extensively studied alkali halide, KCl, at least three lifetime components seem to be present in the spectra, with values in the ranges:  $0.20\text{--}0.25$  nsec ( $\tau_1$ ),  $0.50\text{--}0.65$  nsec ( $\tau_2$ ), and larger than 1 nsec ( $\tau_3$ ). The intensity of the shortest component ( $\tau_1$ ) ranges from 40 to 60%, while the intensity of the longest component ( $\tau_3$ ) is less than 2%. Bertolaccini *et al.*<sup>6</sup> have shown that the annihilation rate of the shortest component can be related to the density of the anions. Several mechanisms have been suggested<sup>7-9</sup> for the processes giving rise to the medium-long component  $\tau_2$ : (a) polaron state of the positron, (b) excited states of a  $\text{Cl}^-e^+$  complex, (c) annihilation at defects, and (d) positron-exciton complex. An important feature of this component is that it exhibits magnetic quenching.<sup>9</sup> The longest lifetime component  $\tau_3$  might be associated with defects, as shown by Nieminen *et al.*<sup>10</sup> in plastically deformed KCl and NaCl.

The interpretation of angular correlation data is also difficult. Stewart and Pope<sup>11</sup> demonstrated that the shape of the angular correlation curve was mainly determined by the anions, and they also found that the measured curves were too narrow when compared to theoretical calculations. More recently, Hautojärvi and Nieminen<sup>4</sup> have

encountered the same discrepancies. Although inadequate models might account for this, it is important to note that considerable radiation damage can build up during angular correlation measurements,<sup>12</sup> hence making a comparison with theory difficult.

In order to gain further insight into the problems outlined above we have performed positron-annihilation-lifetime and Doppler-broadening measurements on thermally quenched potassium-chloride single crystals. The use of the Doppler-broadening technique to obtain the momentum distribution of the annihilation quanta has the advantage over conventional techniques, in that because only very weak positron sources are required, essentially no radiation damage is suffered by the samples.

### II. EXPERIMENTAL

Potassium-chloride single crystals purchased from Harshaw were cleaved and then etched to dimensions  $12 \times 8 \times 0.8$  mm<sup>3</sup>. For the heat treatment the two crystals were wrapped together in aluminum foil and then heated to the desired temperature. The temperature was measured to within  $\pm 2^\circ\text{C}$  by a thermocouple in direct contact with the samples. After 30 min at constant temperature the crystals were quenched in liquid nitrogen, and a positron source, consisting of  $18\text{-}\mu\text{Ci } ^{22}\text{NaCl}$  sealed in  $0.3\text{-mg/cm}^2$  Al foil, was then sandwiched between the two crystals and the assembly mounted in a cryostat. Care was taken to ensure that the same crystal surfaces always faced the positron source.

Lifetime and Doppler-broadened spectra were recorded simultaneously. A conventional fast-slow constant fraction positron lifetime spectrometer was used which had a full-width-at-half-maximum (FWHM) value of the resolution function of

typically 330 psec with  $^{22}\text{Na}$  windows (25 and 70% for the 0.511- and 1.28-MeV windows, respectively), and with slopes of  $\sim 67$  psec. All lifetime spectra were analyzed using the program POSITRONFIT.<sup>13</sup> No source correction was made, and since it is assumed in this program that the resolution function is a Gaussian, the FWHM of the resolution function was determined by a least-squares fitting of one Gaussian to the measured resolution function. Each lifetime measurement was repeated at least once, and each spectrum contained about  $1.6 \times 10^6$  counts.

Doppler-broadening spectra were measured with a digitally stabilized Ge(Li) detector having a resolution function with a FWHM value of 1.5 keV at 0.511 MeV at a counting rate of 4.3 kHz. Again, every measurement was repeated at least once, and each spectrum contained about  $6.5 \times 10^6$  counts accumulated during a time period of 200 min. The spectra were deconvoluted and analyzed using the program DOPPFIT.<sup>14</sup>

### III. RESULTS

All lifetime spectra were first analyzed without any constraints in terms of three components and also in terms of four components ( $\tau_1, \tau_2, \tau_3, \tau_4$  with intensities  $I_1, I_2, I_3$ , and  $I_4$ , respectively). In Table I results are shown for a single representative spectrum. Both types of analysis gave nearly the same  $\chi^2$  values, with only slightly lower values for the four-component fits. The main effect of introducing an additional component is to separate the medium long component  $\tau_2$  in the three-component fit into two individual components ( $\tau_2$  and  $\tau_3$  in the four-component fit). The use of a free four-component analysis resulted in large uncertainties of the parameters, though  $\tau_2$  and  $\tau_3$  (and hence  $I_2$  and  $I_3$ ) were much more uncertain than  $\tau_1, \tau_4, I_1$ , and  $I_4$ . This is due to the fact that  $\tau_2$  and  $\tau_3$  are closer in value to each other than to  $\tau_1$  and  $\tau_4$ . The values of  $\tau_2$  and  $\tau_3$  obtained in these analyses exhibited, for all the measurements (totalling 38), random scatter about the mean values of  $464 \pm 30$  psec ( $\tau_2$ ) and  $774 \pm 45$  psec ( $\tau_3$ ). It therefore seems reasonable to assume that  $\tau_2$  and  $\tau_3$  are constant and the lifetime spectra were therefore reanalyzed using the mean values of  $\tau_2$  and  $\tau_3$  as fixed lifetimes.

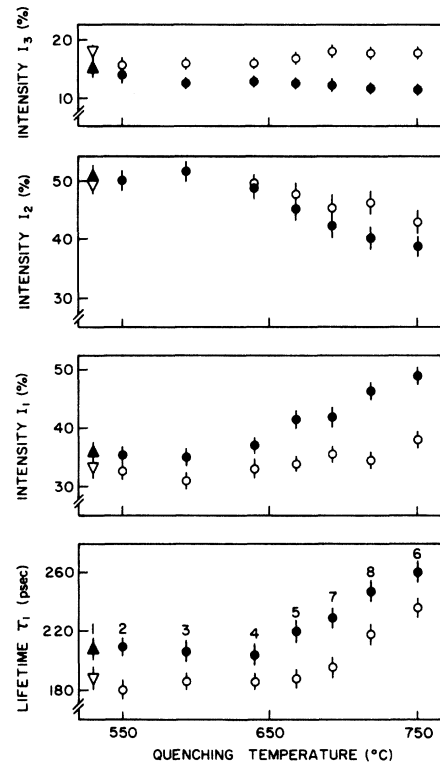


FIG. 1. Lifetime results as a function of quenching temperature with  $\tau_2 = 464$  psec and  $\tau_3 = 774$  psec kept constant. The triangles show results before any quenching. Solid and open symbols are for 90 and 296 °K measurements, respectively.  $\tau_4$  (not shown) had a mean value of 4.4 nsec and  $I_4$  (not shown) the value 0.8% at 90 °K and 2% at 296 °K. The numbers at the  $\tau_1$  values indicate the chronological order of the experiments.

In Fig. 1  $\tau_1, I_1, I_2$ , and  $I_3$  from four-component fits with  $\tau_2$  and  $\tau_3$  fixed are shown as a function of quenching temperature as well as the results obtained before any quenching (triangles). Three different types of measurements were performed for each quenching temperature. The quenched crystals were first measured at 90 °K immediately after the quenching (dots). Then the crystals were allowed to anneal at room temperature for a period of 1–15 h and then cooled again to 90 °K for a new set of measurements. Finally, the crystals were allowed to warm up to room temperature

TABLE I. Computer results of a lifetime spectrum for different numbers of components used in the analysis.

Number of components	$\tau_1$ (psec)	$\tau_2$ (psec)	$\tau_3$ (psec)	$\tau_4$ (psec)	$I_1$ (%)	$I_2$ (%)	$I_3$ (%)	$I_4$ (%)	$\chi^2$
3	$207 \pm 4$	$559 \pm 5$	$3585 \pm 223$	...	$41 \pm 1$	$57 \pm 1$	$2.5 \pm 0.1$	...	1.45
4	$185 \pm 16$	$453 \pm 121$	$694 \pm 197$	$4376 \pm 627$	$33 \pm 6$	$43 \pm 12$	$22 \pm 10$	$2.2 \pm 0.2$	1.43

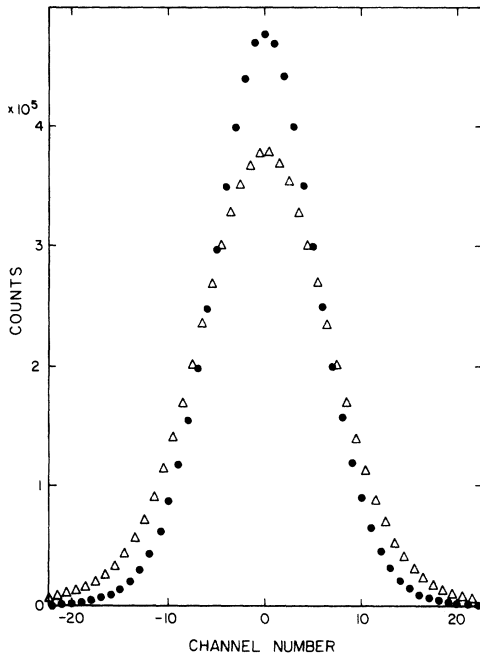


FIG. 2. Doppler-broadened spectrum for measurement No. 2 (see Fig. 1); triangles denote the experimental spectrum while dots show the deconvoluted spectrum. One channel = 0.167 keV = 0.65 mrad.

and measurements were performed at this temperature. The results of these last measurements are shown by the circles. The results for the annealed crystals obtained at 90 °K are not shown in Fig. 1 for clarity. Although they exhibited considerable scatter they all fell in the region spanned by the results for quenched and room-temperature measurements. The lifetime of the longest-lived component  $\tau_4$  (not shown in Fig. 1) had a mean value of  $4.4 \pm 0.2$  nsec with an intensity of  $(2 \pm 0.2)\%$  at 296 °K and  $(0.8 \pm 0.1)\%$  at 90 °K. No

dependence on quenching temperature was observed for this component, to within experimental accuracy. It is clear from Fig. 1 that for the prequenched crystals a small temperature dependence is observed (except for  $I_2$ ) and that the magnitude of this effect is maintained for at least the three lowest quenching temperatures. Furthermore, increasing quenching temperature leads to increasing values of  $\tau_1$  and  $I_1$ , both for quenching and room-temperature measurements, although for the latter to a smaller extent.

We now turn to the Doppler-broadening results. Figure 2 shows a Doppler-broadened spectrum for measurement No. 2 (see Fig. 1) obtained at room temperature (triangles) and the corresponding deconvoluted spectrum (dots). In the analysis of the deconvoluted spectra Gaussians were used for the following reasons: (a) The narrow component was thought to originate from para-Ps decay which is usually represented by a Gaussian. (b) Although it is recognized that the analytical form of any further components is not necessarily Gaussian, it was found that Gaussians constituted a good approximation as deduced from the variance of the fits. The deconvoluted spectra were all analyzed in terms of three Gaussians (characterized by the FWHM parameters  $\Gamma_N$ ,  $\Gamma_{B1}$ , and  $\Gamma_{B2}$  with intensities  $I_N$ ,  $I_{B1}$ , and  $I_{B2}$ , respectively) with no constraints (one-Gaussian and two-Gaussian fits were tried but they gave bad fits), and it was found that the FWHM of the narrow component  $\Gamma_N$  scattered about a value of  $(4.2 \pm 0.2)$  mrad [ $\Gamma(\text{mrad}) = 3.914\Gamma(\text{keV})$ ], and the spectra were then reanalyzed with  $\Gamma_N$  fixed at 4.2 mrad. The results of this analysis are given in Table II, which shows that  $I_N$  decreases, and  $I_{B1}$  increases accordingly, with increasing quenching temperature while no definite dependence is observed for  $\Gamma_{B1}$  and  $\Gamma_{B2}$ .  $I_N$  for "as-quenched" crystals is

TABLE II. Results of three-Gaussian analysis of Doppler-broadened spectra for different quenching temperatures. The measurement numbers refer to the numbers in Fig. 1. The FWHM of the narrow component,  $\Gamma_N$  was fixed at 4.2 mrad.  $\Gamma_{B2}$  had a mean value of 17 mrad. The intensity  $I_{B2}$  is given by  $100 - I_{B1} - I_N$ .  $I_3$  and  $I_4$  are the intensities of the lifetime components  $\tau_3$  and  $\tau_4$ .

Quenching temperature (°C)	Measurement number	As quenched (measured at 90 °K)				Annealed (measured at 296 °K)				
		$I_N$ (%)	$I_{B1}$ (%)	$\Gamma_{B1}$ (mrad)	$(I_3 + I_4)/I_N$	$I_N$ (%)	$I_{B1}$ (%)	$\Gamma_{B1}$ (mrad)	$(I_3 + I_4)/I_N$	
As received	1	$4.7 \pm 0.5$	$91.9 \pm 0.5$	$8.52 \pm 0.07$	$3.4 \pm 0.7$	$7.7 \pm 0.5$	$88.2 \pm 0.5$	$8.53 \pm 0.07$	$2.6 \pm 0.3$	
551	2	4.6	92.0	8.52	3.2	7.6	88.4	8.53	2.4	
594	3	4.6	92.0	8.55	2.9	7.8	88.9	8.56	2.3	
640	4	4.4	91.9	8.59	3.1	7.2	88.1	8.54	2.5	
668	5	3.8	93.5	8.59	3.4	6.5	89.1	8.50	3.1	
697	7	4.0	92.3	8.59	3.3	7.0	88.7	8.65	2.7	
717	8	4.0	93.2	8.63	3.1	6.5	90.4	8.88	3.0	
750	6	3.3	93.0	8.61	3.6	6.0	90.3	8.60	3.3	

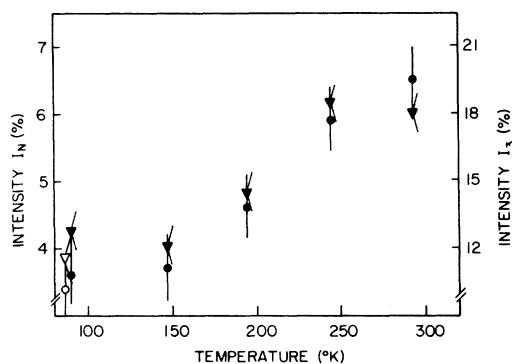


FIG. 3. Intensity  $I_N$  (dots) of narrow component of Doppler-broadened spectra and intensity  $I_3$  (triangles) of lifetime spectra, as a function of temperature. The crystals were annealed. The open symbols show the "as-quenched" results (measurement No. 8, Fig. 1) obtained before the annealing.

seen to be substantially lower than for room-temperature measurements.

With the purpose of investigating further the temperature effect observed for prequenched crystals (see Fig. 1), a series of measurements at different temperatures varying from 90 to 296 °K was performed after annealing at 296 °K for about 15 h the crystals quenched from 717 °C (measurement No. 8 in Fig. 1). In Fig. 3 the results for  $I_3$  and  $I_N$  show that both intensities have essentially the same dependence on temperature (N.B., the scale for  $I_3$  is three times the scale for  $I_N$ ). For the sake of comparison the values for "as-quenched" crystals are shown by open symbols. The rest of the lifetime results are shown in Table III. From this table and Fig. 3 it appears that a significant difference between quenched and annealed crystals (both measured at 90 °K) is found only for  $\tau_1$ ,  $I_1$ , and  $I_2$ , while only little difference is present for  $I_3$ ,  $I_4$ , and  $I_N$ .

#### IV. DISCUSSION

Before discussing the experimental results in detail it is pertinent first to comment on the use of a four-component fit to the lifetime spectra. The choice between a three-component and a four-component fit cannot be made on the basis of the goodness of fit ( $\chi^2$  test, see Table I) since the two fits both have essentially the same values. Our only feasible way to pursue, then, is to make the decision on the basis of "internal" consistency between lifetime and Doppler-broadening analysis. The Doppler-broadened spectra all contain a narrow component with a width of 4.2 mrad and an intensity of (6–8)% at room temperature (Table II), and since magnetic quenching is also observed<sup>9, 15</sup> the narrow component must be due to annihilation of para-positronium (para-Ps). The pick-off annihilation of ortho-Ps should then show up in the lifetime spectra with an intensity of  $3I_N = (18-24)\%$  (disregarding for the moment pick-off annihilation of para-Ps). Such a component is found in four-component fits (see Table I), but not in three-component fits, and from the two  $(I_3 + I_4)/I_N$  columns in Table II as well as from Fig. 3 it is evident that the expected value of  $(I_3 + I_4)/I_N \approx 3$  is found for all measurements. Having thus justified the use of a four-component fit we will proceed by discussing the effect of the thermal quenching, and then later on return to a further discussion of the positronium formation.

##### A. Effect of thermal quenching

It is clear from Fig. 1 that increasing quenching temperature, and thus increasing vacancy concentration, leads to an increase of  $I_1$  and  $\tau_1$ , while  $I_2$  and  $I_3$  decrease. This suggests that  $I_1$  contains a contribution from positron trapping in vacancies, in which the positron annihilates with a lifetime close to, but larger than, the shortest life-

TABLE III. Lifetime results for various temperatures. The results in the first row are for "as-quenched" crystals for measurement No. 8. The crystals were then annealed at 296 °K and thereafter measured at the temperatures indicated. The values of  $I_3$  are shown in Fig. 3.

Measuring temperature (°K)	$\tau_1$ (psec)	$I_1$ (%)	$I_2$ (%)	$I_4$ (%)	Remarks
90	248 ± 6	47 ± 2	41 ± 2	0.8 ± 0.2	As quenched
90	231	40	46	0.6	Annealed
147	230	41	46	0.9	Annealed
194	228	40	44	1.4	Annealed
244	224	37	42	2.0	Annealed
296	218	35	45	1.9	Annealed

time observed for unquenched crystals. We have chosen to analyze these results in terms of a simple statistical model<sup>16</sup> for the annihilation of the positrons, since this model has proven successful in connection with analysis of lifetime spectra for colored KCl.<sup>3, 17</sup> Disregarding  $I_4$  (as it only amounts to  $\sim 0.8\%$ ) one can write down the expression for the intensities:

$$I_1 = (b + \sigma_V n_V) / (K + \sigma_V n_V) + \frac{1}{3} I_3, \quad (1)$$

$$I_2 = c / (K + \sigma_V n_V), \quad (2)$$

$$I_3 = \frac{3}{4} d / (K + \sigma_V n_V), \quad (3)$$

where

$$K = b + c + d, \quad (4)$$

$b$ ,  $c$ , and  $d$  are those parts of the capture cross section per unit volume,  $K$ , which give rise to  $\tau_1$ ,  $\tau_2$ , and  $\tau_3$ , respectively;  $\sigma_V$  is the capture cross section for positron capture in a vacancy; and  $n_V$  is the vacancy concentration. In writing Eqs. (1)–(3) we have used the observation that  $I_1$  increases with quenching temperature and that  $I_3$  is associated with positronium decay (q.v.). It is easy to deduce from (1)–(3) the expressions

$$I_3/I_2 = \text{const} = I_3^0/I_2^0, \quad (5)$$

$$\ln(I_1/I_2 - I_1^0/I_2^0) = \ln(\sigma_V A/b) - E_V^F/kT, \quad (6)$$

using  $n_V = A \exp(-E_V^F/kT)$ , where  $A$  is a constant and  $E_V^F$  is the vacancy formation energy.  $I_1^0$  denotes the initial value of  $I_1$  before any heat treatment. The assumed constancy of the ratio  $I_3/I_2$  is indeed found for all the quenching temperatures (cf. Table IV); this confirms that  $I_2$  and  $I_3$  are not associated with vacancies. The linear relation between  $\ln(I_1/I_2 - I_1^0/I_2^0)$  and  $1/T$  is verified in Fig. 4; the slope of this line gives the vacancy formation energy  $E_V^F = 1.06 \pm 0.1$  eV, and thereby a Schottky-defect formation energy (i.e., the formation energy of an anion and a cation vacancy) of  $2.1 \pm 0.2$  eV in good agreement with the values 2.3–2.5 eV found by conductivity and diffusion methods.<sup>18, 19</sup> Since positrons are not expected to be sensitive to anion vacancies because of their positive charge, the formation energy  $E_V^F$  found here is the cation-vacancy formation energy. For the sake of completeness it should be noted that the Schottky-defect formation energy  $E_S^F$  is only

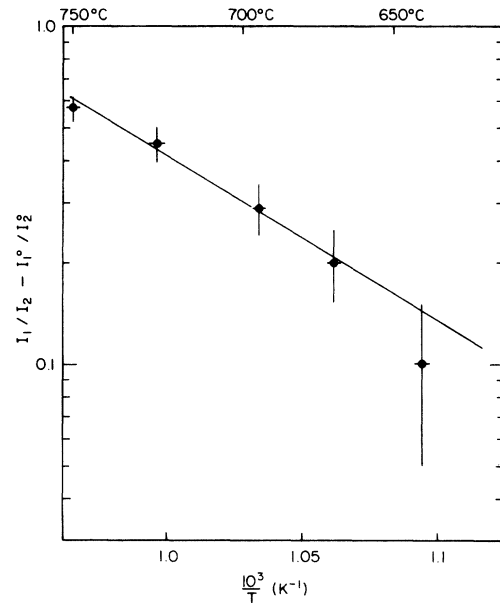


FIG. 4. Arrhenius plot of  $I_1/I_2 - I_1^0/I_2^0$  [see Eq. (6) in text].

given by  $2E_S^F$ , as assumed above, if we have pure crystals, while divalent cation impurities (the most likely divalent impurity type) at high quenching temperatures will result in slightly too low a value of  $E_S^F$ .<sup>20</sup>

The agreement between the two different determinations of  $E_S^F$  can also be taken as an indication of a sufficiently rapid quenching of the surface region (of thickness 0.1–0.2 mm) probed by the positrons. From this point of view the positron-annihilation technique has an advantage over methods which use the entire bulk of a specimen (e.g., resistivity measurements) since it is very difficult to obtain a high quenching rate in the interior of a specimen.

The gradual increase in  $\tau_1$  with quenching temperature was interpreted as being due to an increasing amount of positrons annihilating in vacancies. Denoting the rate of annihilation in vacancies by  $\lambda_V$ , the measured mean annihilation rate  $\bar{\lambda}$  ( $= 1/\tau_1$ ) can be estimated<sup>16</sup> as

$$\bar{\lambda} = (I_1' \lambda_1 + I_V \lambda_V) / (I_1' + I_V), \quad (7)$$

where  $I_V = \sigma_V n_V / (K + \sigma_V n_V)$  is the vacancy contribu-

TABLE IV.  $I_3/I_2$  values for the eight sets of measurements as calculated for "as-quenched" crystals. The model (see text) predicts a constant value.

Measurement number	1	2	3	4	5	6	7	8
$I_3/I_2$	$0.30 \pm 0.02$	0.28	0.26	0.28	0.28	0.29	0.29	0.29

tion to  $I_1$  and  $I_1' = b/(K + \sigma_V n_V) = I_1 - I_V$ .  $\lambda_1$  is the annihilation rate with no vacancies present, which we take as  $1/\tau_1^0 = \frac{1}{207}$  psec<sup>-1</sup>, according to Fig. 1. Fitting  $1/\bar{\lambda}$  by use of (7) to the measured  $\tau_1$  values by assuming different  $\lambda_V$  values we find for the best fit  $1/\lambda_V = \tau_V \approx 340$  psec. Although this determination is not very accurate because the upper-limit value of  $\bar{\lambda}$  ( $=\lambda_V$ ) has not been achieved in the measurements, we feel that the result is sufficiently reliable to contradict the suggestion by Brandt<sup>6</sup> that the 500–650-psec component observed in three-term fits is at least partly due to annihilation in vacancies. Finally, we may calculate the relative positron capture cross section of the vacancies. Using (1) and (2) it is easy to show that

$$\sigma_V n_V / K = I_1^0 (I_1 I_2^0 / I_2 I_1^0 - 1).$$

To determine  $\sigma_V / K$  requires knowledge of the vacancy concentration  $n_V = A \exp(-E_V^F / kT)$ .  $E_V^F$  was determined above, but the preexponential factor  $A$  must be taken from independent work. Using Fuller's<sup>18</sup> result  $A = 43.9$ , giving  $n_V$  in mole fractions, one gets

$$\sigma_V / K = (4_{-3}^{+6}) \times 10^{-19} \text{ cm}^3.$$

An alternative value can be obtained if we write  $K = b + c + d = n_{\text{Cl}^-} (\sigma_b + \sigma_c + \sigma_d)$ , where  $n_{\text{Cl}^-}$  is the number of Cl<sup>-</sup> ions per cm<sup>3</sup>. This gives

$$\sigma_V / (\sigma_b + \sigma_c + \sigma_d) = (1.6_{-1.2}^{+2.4}) \times 10^3,$$

which expresses the relative vacancy trapping cross section to the sum of all other annihilation modes. It turned out, however, that for the higher values of  $E_V^F$  (1.06–1.16 eV)  $\sigma_V / K$  was not constant, so from the model point of view, which assumes a constant ratio, more emphasis should be put on the lower values of  $\sigma_V / K$ , and thereby on the lower values of  $E_V^F$ . The value of  $\sigma_V / K$  is found to be one order of magnitude less than for positron trapping in  $F$  centers<sup>12</sup> ( $\sigma_F / K = 1 \times 10^{-18} \text{ cm}^3$ ).

Compared to metals, the vacancies in KCl are far less effective traps. At 750 °C the vacancy concentration in KCl is about 260 ppm and about 21% of the positrons are trapped herein, while in, e.g., aluminum it only takes about 3 ppm to trap the same amount, as calculated from the results of McKee *et al.*<sup>21</sup> In other words, vacancies in KCl are about a factor of  $10^2$  less effective as traps. This allows us to make a rough estimate of the binding energy of positrons to vacancies in KCl using Brandt's<sup>22</sup> calculations. He finds that the ratio between the trapping rates in insulators and metals is given by the approximate expression  $(\pi^2 \lambda_+ / 2r_d) (\Gamma / E_B)$ , which in our case has the value  $10^{-2}$ .  $\lambda_+$  is the de Broglie wavelength of the positron and  $r_d$  the effective radius of the trapping

potential.  $\Gamma$  is the damping width given by  $2\pi\Gamma \sim kT$  and  $E_B$  the binding energy. We take  $2r_d = 5 \text{ \AA}$  which is the value normally used for the square-well diameter for  $F$  centers in KCl, and with  $T = 90 \text{ }^\circ\text{K}$  one gets  $E_B \approx 2 \text{ eV}$ . This is less by a factor of 2 or 3 than calculated for most metals.<sup>22</sup>

We will only briefly consider the effect of annealing of the quenched samples since this was not the primary aim of this work. The values of  $\tau_1$ ,  $I_1$ , and  $I_2$  measured at room temperature (c.f. Fig. 1) indicate that only a partial annealing has taken place, since the values of these parameters deviate from those pertinent to prequenched (i.e., truly annealed) crystals. These deviations increase, as expected, with increasing quenching temperature and since monovacancies are mobile at room temperature it is hence suggested that we here observe the effects of vacancy cluster formation. A similar conclusion with respect to vacancy cluster formation was arrived at by Mitchell *et al.*<sup>23</sup> on the basis of color-center work.

#### B Positronium formation and temperature dependence

In the beginning of the discussion the association of  $I_3$  and  $I_N$  to annihilation of Ps was made, and since magnetic quenching of the longest-lived component  $\tau_4$  has been observed by Bisi *et al.*,<sup>9</sup> we will in the following incorporate this component in the Ps formation yield. The ratio  $(I_3 + I_4) / I_N$  can then be written, taking into account pick-off annihilation of para-Ps:

$$(I_3 + I_4) / I_N = 3(\lambda_s + \lambda_3^p + \lambda_4^p) / \lambda_s, \quad (8)$$

where  $\lambda_s$  is the annihilation rate of para-Ps and  $\lambda_3^p = 1/\tau_3$  and  $\lambda_4^p = 1/\tau_4$  the pick-off rates of ortho-Ps. Using first the vacuum value of  $\lambda_s$  ( $\frac{1}{125} \text{ psec}^{-1}$ ), (8) becomes  $(I_3 + I_4) / I_N = 3.5$ . The experimental data have a mean value of  $3.3 \pm 0.2$  at 90 °K and  $2.7 \pm 0.4$  at room temperature, which, considering the rather complex analysis of the data, is in reasonable agreement with the theoretical value. If, instead of using the vacuum value for  $\lambda_s$ , one uses the value predicted for relaxed Ps, as discussed by Bisi *et al.*,<sup>9</sup> the para-Ps annihilation rate is  $\lambda_s = \alpha / 125 \text{ psec}^{-1}$ ,  $\alpha$  being the relaxation parameter. They find  $\alpha = 0.3$  from magnetic quenching of lifetime spectra [and (8) then has the value 4.9], while our data indicate that  $\alpha \approx 1$ , in agreement with Smedskjaer and Dannefaer,<sup>15</sup> who used magnetic quenching of angular correlation spectra. A significant discrepancy between the two determinations of  $\alpha$  is evident and at present we are unable to explain this. A further confirmation that  $I_3$  and  $I_4$  arise from Ps annihilation is possible by considering the yield for 3- $\gamma$  annihila-

tion; Bisi *et al.*<sup>24</sup> measured the yield  $P_{3\gamma}$  to be  $(3.50 \pm 0.08) \times 10^{-3}$  at room temperature; and using Eq. (22) in Ref. 25 one finds from our lifetime data  $P_{3\gamma}$  (calc) to be  $(3.6 \pm 0.2) \times 10^{-3}$  [if  $I_4$  is omitted, then  $P_{3\gamma}$  (calc) =  $(3.0 \pm 0.05) \times 10^{-3}$ ].

It was pointed out in Sec. I that angular correlation curves were narrower than the theoretical curves and we can now see at least one reason for this, namely that Ps formation is occurring. In this regard we will restrict ourselves to a comparison between the calculation of Hautojärvi and Nieminen<sup>4</sup> and our Doppler-broadening results (Fig. 5). Two contributions to the momentum distribution arising from positrons in  $1s$  or  $2p$  states were calculated in their model, both giving substantially broader distribution than the angular correlation data. The solid line shows the result obtained from Doppler broadening with the narrow component subtracted, since Ps formation is not considered in their model, and a significantly better agreement with theory is observed. A similar conclusion was reached when comparing Stewart and Pope's<sup>11</sup> results. Furthermore, it is pointed out that even if the narrow component is not subtracted the Doppler-broadened spectra are still less narrow than the angular correlation data, which might be a consequence of the substantial radiation damage suffered by samples exposed to the relatively strong angular correlation sources.

The cause of the temperature dependence of the Ps yield, i.e.,  $I_3$ ,  $I_4$ , and  $I_N$  as shown in Fig. 3 and Table III, is not clear, and only a tentative explanation can be offered at this point. When Ps is formed a certain amount of energy (a few electron volts) is given up to the lattice. Since KCl

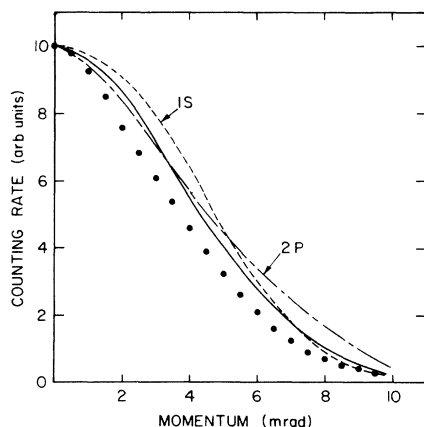


FIG. 5. Momentum distribution calculated from Doppler-broadened spectra with the narrow component subtracted (solid line). Theoretical curves denoted  $1S$  and  $2P$  are from Ref. 4 ( $1S$  and  $2P$  refer to two states of the positron). Angular correlation data from Ref. 4 are shown by the dots.

has a band gap of 7–8 eV, electron-hole pairs cannot be formed so the binding energy is carried away by phonons (this is contrary to metals where electron-hole pair formation is the predominant mechanism of energy dissipation). In order to explain qualitatively the temperature dependence, use has been made of the calculations by Thornber and Feynman<sup>26</sup> of the rate of energy loss of polarons. We envisage simply that the binding energy of Ps is first transformed into kinetic energy which is then lost by phonon interactions and further, that a high rate of energy dissipation makes the Ps atom less likely to break up than if the rate is low. The binding energy  $E_B$  as mentioned before, is a few electron volts, which means that we are concerned with the high-energy limit in Thornber and Feynman's diagrams<sup>26</sup> ( $E_B \gg \hbar\omega_{LO}$ , where  $\hbar\omega_{LO}$  is the energy of longitudinal-optical phonon mode, which in KCl is<sup>27</sup> 0.028 eV). In this limit the rate of energy loss decreases with increasing inverse temperature,  $\beta = \hbar\omega_{LO}/kT$  but for  $\beta$  larger than  $\sim 3$  it stays approximately constant ( $\beta \geq 3$  corresponds in KCl, to a temperature of  $\leq 110^\circ\text{K}$ ). This would explain the low constant value of  $I_3$  and  $I_N$  at temperatures less than  $150^\circ\text{K}$ , as well as the increase with temperature. At higher temperatures ( $> 250^\circ\text{K}$ ) constant values are again obtained, which could be explained by assuming that the energy dissipation rate now is so high that all the Ps formed manages to survive and hence the amount is determined by the probability that Ps is formed in the first place.

Finally we consider briefly if Ps formation is an intrinsic property of KCl, i.e., if Ps is formed in perfect KCl. First, it follows from Fig. 1 that vacancies are not necessary for the formation of Ps since  $I_3$  decreases with increasing vacancy concentration, and second, considering Brandt's<sup>2</sup> results on  $\text{Ca}^{++}$ -doped KCl, it seems unlikely that impurities could cause Ps formation in nominally pure crystals. Both observations thus suggest that Ps formation is an intrinsic property of KCl, in agreement with recent Ore-gap calculations.<sup>28</sup> From the FWHM of the narrow component (4.2 mrad) it follows, using the Heisenberg uncertainty principle, that the Ps atom is confined in a space with an expectation diameter of  $2 \text{ \AA}$ . Since Ps is not formed in vacancies this space would likely be an interstitial position.

It has been established that  $\tau_3$  and  $\tau_4$  are physically due to Ps formation. However, with a value of 4.4 nsec for  $\tau_4$  it is difficult to understand if this would arise from a process in the "bulk" of the material. It might instead arise from surface states of positronium.

It is still difficult to define  $\tau_2$  and that part of  $\tau_1$  not due to trapping in vacancies in terms of spe-

cific physical processes. It has been suggested that these two components could arise from different states of the  $\text{Cl}^-e^+$  complex. In that case one might expect the same temperature dependence of  $I_1$  and  $I_2$  but according to Table III  $I_2$  remains roughly constant while  $I_1$  increases with decreasing temperature. In this connection the contributions to  $I_1$  from para-Ps decay (amounting to  $\frac{1}{3}I_3$ ) should actually be subtracted, which then would lead to a stronger temperature dependence of  $I_1$ . In agreement with Bertolaccini *et al.*<sup>1</sup> it is hence suggested that the two lifetimes  $\tau_1$  and  $\tau_2$  are of different physical nature. Since a positron trapped in a vacancy probably annihilates with an electron from the surrounding  $\text{Cl}^-$  ions and since  $\tau_V$  obeys the inequalities  $\tau_1 < \tau_V < \tau_2$  we put forward the hypothesis that  $\tau_1$  arises from annihilation with  $\text{Cl}^-$  ions. As to the physical nature of  $\tau_2$  the present experiments do not yield any conclusive information. However, if we restrict ourselves to the annihilation mechanisms noted in the Introduction we can rule out case (b) (excited states of a  $\text{Cl}^-e^+$  complex), case (c) (annihilation at defects), and case (d) (positron-exciton complex). The different temperature dependence of  $I_1$  and  $I_2$  rules out case (b), and since annihilation at defects takes place with a lifetime of  $\sim 340$  psec this rules out case (c). Finally we rule out case (d) since the positron-exciton complex is expected to have a small center-of-mass momentum which would contribute to the narrow component in the Doppler-broadened spectra. Furthermore, Nieminen<sup>29</sup> has calculated that a positron-exciton complex is not stable in KCl. We therefore suggest that the  $\tau_2$  component is associated with a polaron state of the positron. This is substantiated by the calculations of Goldanskii and Prokop'ev,<sup>7</sup> who find a lifetime of about 500 psec in good agreement with our value of 464 psec.

## V. SUMMARY

It has been shown in this work that at least four lifetime components are present in KCl. The two shortest-lived components with lifetimes 200 and 464 psec are not connected with annihilation of positronium. It is suggested that the 200-psec component arises from annihilation with  $\text{Cl}^-$  ions, and that the 464-psec component from a polaron state of the positron. The two longest-lived components with lifetimes 773 and 4400 psec arise from positronium annihilation.

From thermal-quenching experiments in the range 550–750 °C, it has been demonstrated, using a simple statistical model for the annihilation processes, that vacancies trap positrons at which the positron annihilate with a lifetime of about 340 psec. Further, the formation energy of Schottky defects was deduced to be about 2.1 eV. By comparison with the trapping efficiency of vacancies in metals, the binding energy of a positron to a vacancy in KCl was found to be roughly 2 eV.

With regard to positronium formation it was found that the ratio between the intensities of the "positronium" components in lifetime spectra and the intensity of the narrow component in Doppler-broadened spectra had a value close to 3, indicative of formation of unrelaxed positronium. Also, it was observed that the positronium formation yield was strongly dependent on temperature (16% at  $T < 150$  °K and 25% at  $T > 250$  °K). This dependence has been explained by assuming that the probability of breaking up of formed positronium depends on the rate of energy dissipation (by phonons) of the binding energy.

## ACKNOWLEDGMENT

We are indebted to Dr. D. P. Kerr for his cooperation during this work.

\*Work supported by the National Research Council of Canada.

<sup>1</sup>M. Bertolaccini and A. Dupasquier, *Phys. Rev. B* **1**, 2896 (1970).

<sup>2</sup>W. Brandt and H. F. Waung, *Phys. Rev. B* **3**, 3432 (1971).

<sup>3</sup>S. Dannefaer, G. Trumpy, and R. M. J. Cotterill, *J. Phys. C* **7**, 1261 (1974).

<sup>4</sup>P. Hautojärvi and R. Nieminen, *Phys. Status Solidi B* **56**, 421 (1973).

<sup>5</sup>W. C. Mallard and F. H. Hsu, in *Second International Conference on Positron Annihilation*, Kingston, Canada, 1971 (unpublished).

<sup>6</sup>M. Bertolaccini, A. Bisi, G. Gambarini, and L. Zappa, *J. Phys. C* **4**, 734 (1971).

<sup>7</sup>V. I. Goldanskii and E. P. Prokop'ev, *Fiz. Tverd. Tela* **6**, 3301 (1964) [*Sov. Phys.—Solid State* **6**, 2641 (1965)].

<sup>8</sup>W. Brandt, in *Positron Annihilation*, edited by A. T. Stewart and L. O. Roellig (Academic, New York, 1967).

<sup>9</sup>A. Bisi, A. Dupasquier, and L. Zappa, *J. Phys. C* **6**, 1125 (1973).

<sup>10</sup>R. Nieminen, P. Hautojärvi, and P. Jauho, *Appl. Phys.* **5**, 41 (1974).

<sup>11</sup>A. T. Stewart and N. K. Pope, *Phys. Rev.* **120**, 2033 (1960).

<sup>12</sup>S. Dannefaer and L. Smedskjaer, *J. Phys. C* **6**, 3536 (1973).

<sup>13</sup>P. Kirkegaard and M. Eldrup, *Comput. Phys. Commun.* **3**, 240 (1972).

<sup>14</sup>S. Dannefaer and D. P. Kerr, *Nucl. Instrum. Methods*



- 131, 119 (1975).
- <sup>15</sup>L. Smedskjaer and S. Dannefaer, *J. Phys. C* 7, 2603 (1974).
- <sup>16</sup>R. N. West, *Adv. Phys.* 22, 263 (1973).
- <sup>17</sup>S. Dannefaer, D. P. Kerr, and B. G. Hogg, *J. Phys. C* 8, 2667 (1975).
- <sup>18</sup>R. G. Fuller, *Phys. Rev.* 142, 524 (1966).
- <sup>19</sup>R. G. Fuller, C. L. Marquardt, M. H. Reilly, and T. C. Wells, Jr., *Phys. Rev.* 176, 1036 (1968).
- <sup>20</sup>R. G. Fuller, in *Point Defects in Solids*, edited by J. H. Crawford, Jr. and L. M. Slifkin (Plenum, New York, 1972), Vol. 1.
- <sup>21</sup>B. T. A. McKee, W. Trifthäuser, and A. T. Stewart, *Phys. Rev. Lett.* 28, 358 (1972).
- <sup>22</sup>W. Brandt, *Appl. Phys.* 5, 1 (1974).
- <sup>23</sup>P. V. Mitchell, D. A. Wiegand, and R. Smoluchowski, *Phys. Rev.* 121, 484 (1961).
- <sup>24</sup>A. Bisi, C. Bussolati, S. Cova, and L. Zappa, *Phys. Rev.* 141, 348 (1966).
- <sup>25</sup>V. I. Goldanskii, in Ref. 8.
- <sup>26</sup>K. K. Thornber and R. P. Feynman, *Phys. Rev. B* 1, 4099 (1970).
- <sup>27</sup>R. P. Lowndes, *Phys. Lett.* 21, 26 (1966).
- <sup>28</sup>G. M. Bartenev, A. Z. Varisov, A. V. Ivanova, M. N. Pletnev, E. P. Prokop'ev, and A. D. Tsyganov, *Fiz. Tverd. Tela* 14, 715 (1972) [*Sov. Phys.-Solid State* 14, 608 (1972)].
- <sup>29</sup>R. Nieminen, Cavendish Laboratory, Report No. TCM/6/1975, Cambridge, England (unpublished).